Ain Shams Engineering Journal 15 (2024) 102584

Contents lists available at ScienceDirect

Ain Shams Engineering Journal

journal homepage: www.sciencedirect.com

Numerical investigation of thermal performance enhancement of pin fin heat sink using wings with different angles

Mostafa A.H. Abdelmohimen [a,*], Mostafa A. Hussien [b], Salem Algarni [b], Mohamed A. Karali [c], C. Ahamed Saleel [b], Gulam M.S. Ahmed [d,e], H.A. Refaey [f,a]

[a] Department of Mechanical Engineering, Faculty of Engineering at Shoubra, Benha University, 11629 Cairo, Egypt
[b] Mechanical Engineering Department, College of Engineering, King Khalid University, Abha 61421, Saudi Arabia
[c] Department of Mechanical Engineering, Faculty of Engineering and Technology, Future University in Egypt, New Cairo, Egypt
[d] Department of Mechanical Engineering, Adama Science and Technology University, Adama, Ethiopia
[e] Center of Excellence (COE) for Advanced Manufacturing Engineering, Program of Mechanical Design and Manufacturing Engineering, Adama Science and Technology University, Adama 1888, Ethiopia
[f] Department of Mechanical Engineering, College of Engineering at Yanbu, Taibah University, Yanbu Al-Bahr 41911, Saudi Arabia

A B S T R A C T

The current study represents a numerical investigation of the pin fin heat sink performance with different angles of wings. Five angles ranging from 0° to 90° have been represented and studied under inline and staggered arrangements of pin fins. Reynolds numbers range from 13,500 to 37500. The highest Nusselt number has been achieved by angle-0° with inline arrangement while it has been achieved by angle-22.5° with staggered arrangement. On the other hand, the maximum friction factor with both inline and staggered arrangements is represented by angle-0°. The highest thermohydraulic performance has been achieved by angle-22.5° for staggered arrangement while case without wings gives the highest performance for inline arrangement. Using wings in staggered arrangement shows significant effect on heat transfer performance. While it is not recommended to use wings in case of inline arrangement.

1. Introduction

Recently, more attention has been paid to improve the heat sinks performance. Heat sinks are used in many applications such as electronic equipment, cooling systems, and air-conditioning. Improving the heat sink thermal performance, reduces its size and increases the rate of heat dissipation. Changing the profile and shape of the heat sink fins is considered one of improving performance techniques. The heat sink has an array of fins with different shapes and configurations to increase the heat transfer area. Plate fins and pin fins are examples of commonly used heat sinks. Plate fin heat sinks performance has been investigated and improved by many investigators [1–6]. Hussain et al. [3] investigated the flow direction effect and fillet profile on thermal performance of plate-fin heat sinks. Abdelmohimen et. al. [6] improved the performance of the plate fin heat sink through separating of fins into multi-numbers instead of one slide fin. Pin fin heat sink takes a square, cylindrical, or elliptical cross-section that extends from its base. The heat dissipation from heat sinks depends also on the flow characteristics.

Pressure drop and heat transfer of channels with pin fins of circular or a few different cross sections have been investigated [7–16]. Tahat et al. [8] investigated optimal spacing of the fins in the streamwise and directions of span wise for staggered and inline arrangements of pin fins. Bilen et al. [9] studied the heat transfer characteristics of both staggered and inline arrangements of tube fins. Sara et al. [16] studied the effect of using square cross-section pin fins. They concluded that, better performance can be achieved by using large number of longer pin fins. Perforated pin fin heat sink has been represented to improve thermal performance of pin fin heat sinks [17–19]. Sahin and Demir [17] represent pressure drop and heat transfer for a flat surface fitted with perforated pin fins in a channel has rectangular shape. Their results showed that a heat transfer enhancement due to use of perforated pin fins. Al-Damook et al. [18] showed that the thermal dissipation increases by increasing the perforation on pin fins sink which leads to increase the heat transfer rate on heat sink. Tijani and Jaffri [19] present an opportunity to enhance understanding of the influence of different factors such as temperature distribution, pressure drop, and perforation level on the heat sink thermal performance. Their results show that perforated flat plate and pin fins heat sink improve the thermal efficiency by 1–4 % as compared to solid flat plate and solid pin fins heat sink. Naphon and Sookkasem [20] represented the performance of heat transfer of taper pin fin heat sink. Yuan et al. [21] investigated numerically the plate pin fin heat sink. A significant effect of the air velocity and pin height have been shown on thermo-hydraulic performance. The effect of pin cross-section on pressure drop and heat transfer has been exmined by Sahiti et al. [22]. Choudhary et al. [23] studied

* Corresponding author.

https://doi.org/10.1016/j.asej.2023.102584
Received 24 May 2023; Received in revised form 27 October 2023; Accepted 15 November 2023
Available online 28 November 2023

Nomenclature

A_T	Heat sink total surface area
B	Base height (m)
D	Pin fin diameter (m)
D_h	Hydraulic diameter (m) $D_h = 4Ac/P$
A_c	Cross section area at inlet
f	Friction factor
H	Pin fin height, above the base (m)
$\overline{h}$	Mean heat transfer coefficient
L	Heat sink length (m)
K	Thermal conductivity (W/m.K)
$\dot{m}$	Mass flow rate (kg/s)
N	Number of pins
Nu	Nusselt number
Heat transfer rate	(Watt)
Δp	Pressure drop (Pa)
THP	Thermohydraulic Performance
U_{avg}	Average velocity
W	Width of the heat sink (m)

Greek symbols

ρ_a	density (kg/m^3)
μ_a	viscosity of the air (Pa. s)

Subscripts

a	Air
avr	average
b	Base
in	Inlet
out	Outlet
s	For smooth plate

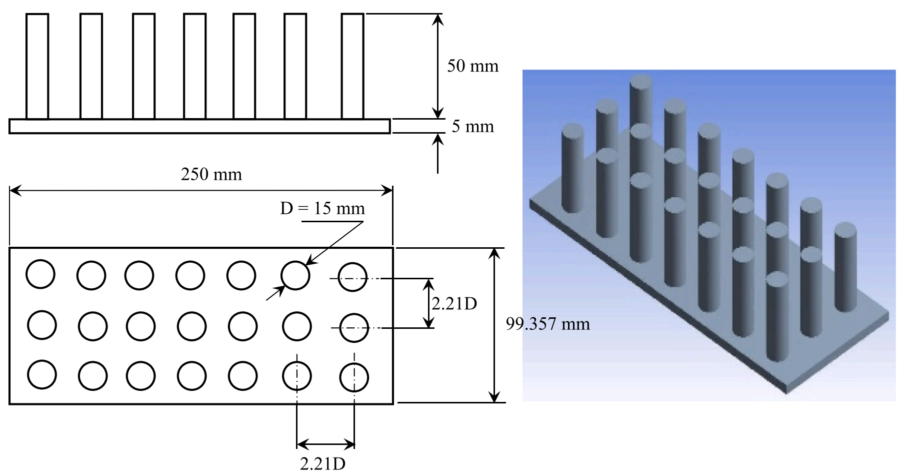

a) Baseline case (case-1) with dimensions for inline arrangement

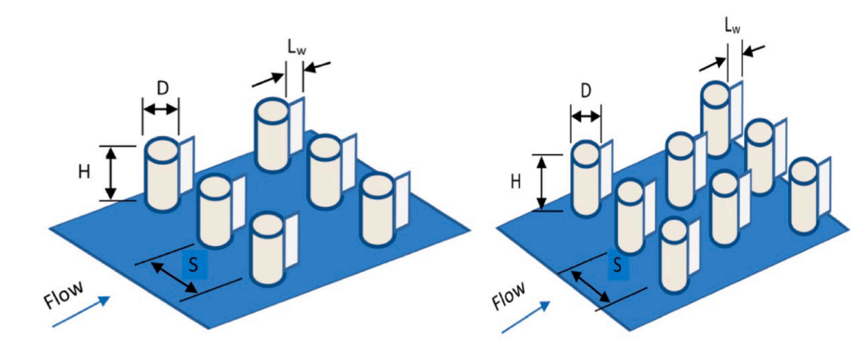

b) Pin fin with wings in inline arrangement [23] c) Pin fin with wings in staggered arrangement [23]

Fig. 1. Pin fin heat sink geometry with dimensions.

experimentally behaviour of air flow and heat transfer on pin fin heat sink with and without wings under forced convection. Staggered and inline arrangements have been studied for various pitch ratio and wing sizes ratio for the Reynolds number range of 6800–15100. They applied wings only at angle 90°.

Souida et al. [24] investigated numerically the effect of the shape of pin fins on the overall performances of heat sinks. Conical shaped pin fins with varying conical size ratio (Hcp/d) are considered. The values of the hydrothermal performance factor (h) for the conical fins are greater than those of the cylindrical fins. Bencherif et al. [25] numerically investigated the effect of the combination between perforation technique and splitters inserts on the heat dissipation and turbulent fluid flow characteristics of pin fins heat sinks. While the heat transfer and fluid flow on a new design of heat exchangers with grooved pin–fin heat

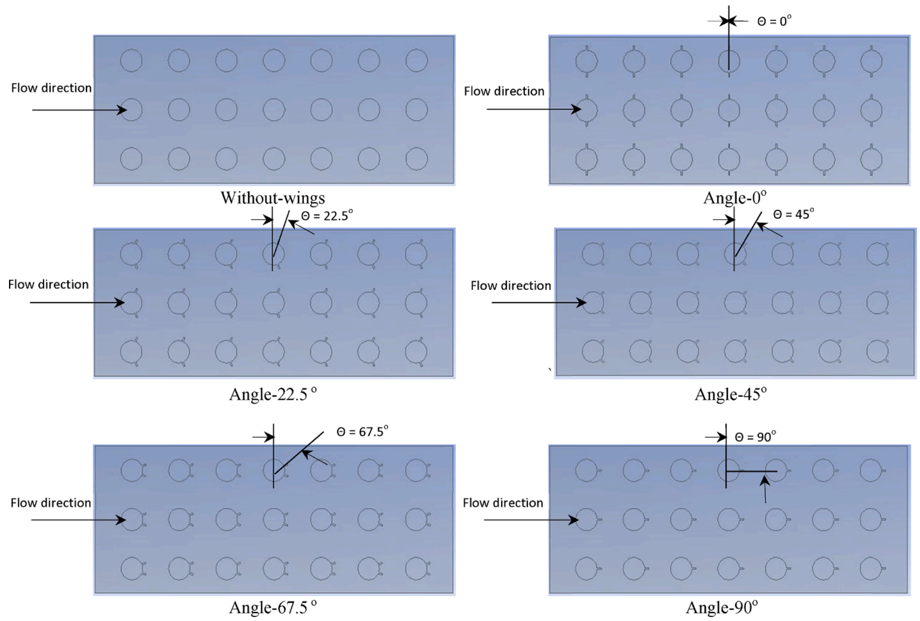

Fig. 2. Studied cases with different angles of wings as represented in inline arrangement.

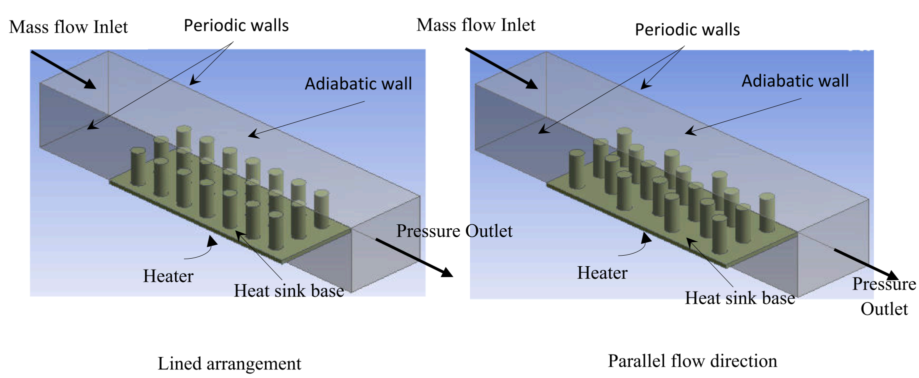

Fig. 3. Studied arrangements with boundary conditions.

sinks have been investigated by Bencherif et al. [26]. Sahel et al. [27] examined the hydrothermal performance of a heat sink having hemispherical pin fins (*HSPFs*) under fully turbulent flow conditions and to find the optimum *HSPFs* configuration.

From literature surveys, it is clear that a few researchers have represented pin fins with wings. However, to the best knowledge of the authors, the effect of using wings attached to pin fins at different angles has not been investigated. Applying wings, without determining the optimum angle at which the maximum thermal performance can be achieved, may be useless. The importance of the current work is to fill this gap and represents a numerical analysis to optimize the best angle of the wings that can be used to give the highest enhancement in the thermal performance of pin fin heat sinks.

2. Numerical simulation

2.1. Studied models

The studied cases depend on attaching wings to the pins of pin fin heat sinks. Fig. 1a. represents the studied pin fin heat sink without attached wings and clears its dimensions. The wing dimensions are Lw = 0.2 D with thickness = 1 mm as shown in Fig. 1b. The selected length of wing gives the highest Nusselt number as compared with larger and smaller lengths according to [23]. The duct height is twice the pin fin height. The ratio between pin fin height and duct height has been chosen because it gives higher thermal efficiency as mentioned by Sahin and Demir [17]. Different angles of wings have been studied. The angle of the wing is measured from the normal axis to the direction of the flow. Five different angles have been studied, namely (0°, 22.5°, 45°, 67.5°, and 90°). Two wings have been attached to the pin on both sides with all studied angles except with 90° angle. Only one wing has been attached in case of 90° angle. Fig. 2 shows the studied pin fin with the studied angled wings. The study has been carried out for inline and staggered arrangements. Fig. 3 shows the studied domain for both inline and staggered arrangements.

2.2. Mesh generation

A grid independency has been carried out to select the suitable mesh. The tested mesh sizes ranged from 688,020 to 2,780,116 for case without wings at Re = 37500. The selected size of mesh is 1,007,399 for the base case. The mesh after added wings reached to 1798591. The change in Nusselt number between the selected mesh and the maximum mesh sized is not more than 4.7 %.

2.3. Boundary conditions and modeling

The boundary conditions are selected to compare the results of the

Table 1
Studied range of Reynolds number and corresponding mass flow rate.

No.	Corresponding *Re*	Mass flow rate (kg/s)
1	13,500	0.024846
2	18,250	0.033588
3	23,000	0.04233
4	28,000	0.051532
5	33,000	0.060734
6	37,500	0.069016

base-case with the experimental results of Sahin and Demir [17] for validation. Six values of Reynolds number have been studied by assuming mass flow rate at inlet with turbulence intensity of 5 %- and 1000-mm turbulence length scale and inlet temperature 25 °C. Table 1 shows the studied mass flow rate and the corresponding Reynolds number. Reynolds number is calculated based on the inlet hydraulic diameter. Eq. (1) is used to calculate Reynolds number. Air properties were taken as dynamic viscosity (μ_a) = 1.8462 x 10^{-5} kg/m.s, density (ρ_a) = 1.1774 kg/m^3, specific heat (cp_a) = 1.0057 x 10^3 J/kg.K, and thermal conductivity (k_a) = 0.02624 W/m.K. The selected material of the heat sink is Aluminum alloy with thermal conductivity (k_s) = 222 W/m K. The heater dimensions are 200 mm length x 99.375 mm width. While the base area of the heat sink is 250 mm length x 99.375 mm width. The heat flux of the heater is assumed to be 4000 W/m^2. The side walls of the duct are assumed to be a periodic wall for symmetry. The up and down walls of the fluid domain are assumed adiabatic walls except the area of the heater. All assumed boundary conditions are shown on Fig. 3.

$$Re_{Dh} = \frac{\rho_a U_{avg} D_h}{\mu_a} \tag{1}$$

Simulation study has been carried out by using Shear-Stress Transport (*SST*) *K-ω* model [5]. The following assumptions have been considered through this study:

1- Three-dimensional, steady, and incompressible air flow.
2- Conjugate heat transfer.
3- Neglect radiative heat transfer from the heat sink.

The used governing equations are as follows:
The continuity equation is given by:

$$\nabla\left(\rho\vec{U}\right) = 0 \tag{2}$$

The *N-S* equations across the x, y, and z directions are given by:

$$\begin{aligned}
\nabla\left(\rho\vec{U}u\right) &= -\frac{\partial p}{\partial x}+\frac{\partial \tau_{xx}}{\partial x}+\frac{\partial \tau_{yx}}{\partial y}+\frac{\partial \tau_{zx}}{\partial z}\\
\nabla\left(\rho\vec{U}v\right) &= -\frac{\partial p}{\partial y}+\frac{\partial \tau_{xy}}{\partial x}+\frac{\partial \tau_{yy}}{\partial y}+\frac{\partial \tau_{zy}}{\partial z}\\
\nabla\left(\rho\vec{U}w\right) &= -\frac{\partial p}{\partial z}+\frac{\partial \tau_{xz}}{\partial x}+\frac{\partial \tau_{yz}}{\partial y}+\frac{\partial \tau_{zz}}{\partial z}
\end{aligned} \tag{3}$$

where ρ is the density of fluid, (u, v and w) are velocity components in three directions, $\vec{U}$ is the velocity, τ is the viscous stress tensor, and p is pressure.

The energy equation is given by:

$$\nabla\left(\rho h\vec{U}\right) = -p\nabla\vec{U}+\nabla(k\nabla T) \tag{4}$$

where h is the aggregate enthalpy, k is thermal conductivity, and T is temperature.

The transport equations for the SST *K-ω* are given by:

$$\frac{\partial}{\partial t}(\rho k)+\frac{\partial}{\partial x_i}(\rho k u_i) = \frac{\partial}{\partial x_j}\left(\Gamma_k\frac{\partial k}{\partial x_j}\right)+G_k-Y_k+S_k \tag{5}$$

$$\frac{\partial}{\partial t}(\rho\omega)+\frac{\partial}{\partial x_i}(\rho\omega u_i) = \frac{\partial}{\partial x_j}\left(\Gamma_\omega\frac{\partial \omega}{\partial x_j}\right)+G_\omega-Y_\omega+D_\omega+S_\omega \tag{6}$$

Where G_k represents the generation of turbulence kinetic energy due to mean velocity gradients and G_ω represents the generation of ω and they calculated as follows:

$$G_k = -\rho\overline{u_i' u_j'}\frac{\partial u_j}{\partial x_i} \tag{7}$$

$$G_\omega = \alpha\frac{\omega}{k}G_k \tag{8}$$

And, Γ_k and Γ_ω represent the effective diffusivity of k and ω, respectively. Y_k and Y_ω represent the dissipation of k and ω due to turbulence. D_ω represents the cross-diffusion term. S_k and S_ω are user-defined source terms.

3. Calculation procedure

To represent the performance of the heat sinks, average Nusselt number and friction factor should be calculated. Eq. (9) is used to calculate Nusselt number.

$$\overline{Nu} = \frac{\overline{h}D_h}{k} \tag{9}$$

Where D_h is the hydraulic diameter based on the duct inlet area, $\overline{h}$ is the average heat transfer coefficient, and k is the air thermal conductivity determined at the average temperature (T_{avg}) where T_{avg} can be calculated as:

$$T_{avg} = \frac{T_{in}+T_{out}}{2} \tag{10}$$

Where T_{in} and T_{out} are the inlet and outlet temperature respectively. The average heat transfer coefficient is calculated by using Eq. (11)

$$\overline{h} = \frac{Q}{A_T(T_b - T_{avg})} \tag{11}$$

Where Q is the heat transfer rate calculated by Eq. (12), T_b is the fin base temperature, and A_T is the total heat sink area subjected to the fluid flow. Two equations are used to calculate the total area. The first one is used to calculate the total area for pin fin heat sink without wings. While the second one is used to calculate the total area with wings.

$$Q = \dot{m}_a C_p(T_{out} - T_{in}) \tag{12}$$

$$A_{T_{withoutwings}} = WL + N\pi DH \tag{13}$$

$$A_{T_{withwings}} = (WL+N\pi DH)+2N((L_w{*}t_w)+2L_w{*}H) \tag{14}$$

Where $\dot{m}_a$ and C_p are the mass flow rate (kg/s) and specific heat of air at the average temperature respectively. L and W are the length and width of the heat sink respectively, N, D, and H are the fins number, pin fin diameter, and height above the base respectively. For fins with wings, L_w and t_w are the wing length and thickness respectively. The wing has the same height of the pin fin. Note that in case of 90o angle, the pin fin have only one wing instead of two wings and in this case th (*2 N*) in equation (14) becomes (*N*).

The friction factor is calculated based on the pressure drop Δp through the heat sink. Eq. (15) is used to calculate the friction factor.

$$f = \frac{2\Delta p D_h}{\rho U_{avg}^2 L} \tag{15}$$

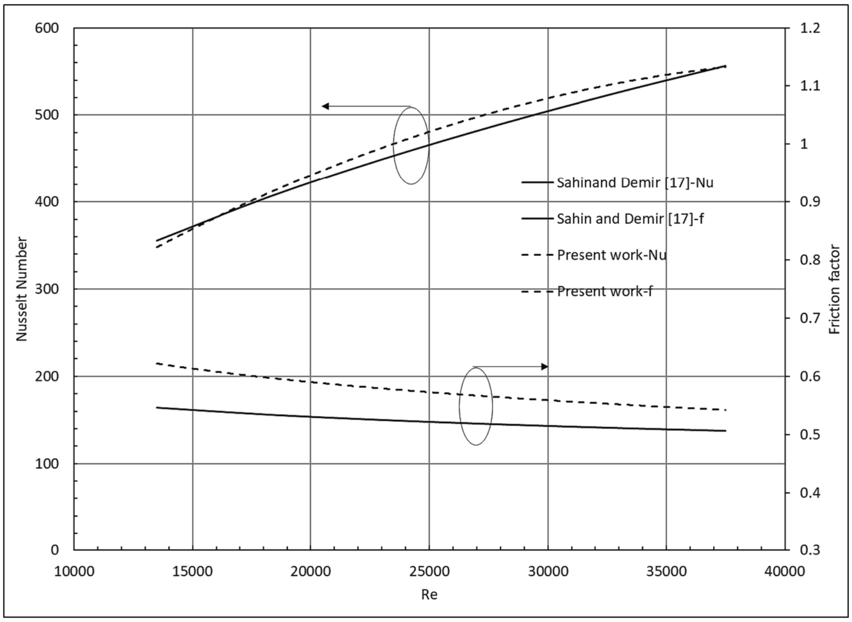

Fig. 4. Validation of present work for Nusselt number and friction factor with pin fin heat sink without wings.

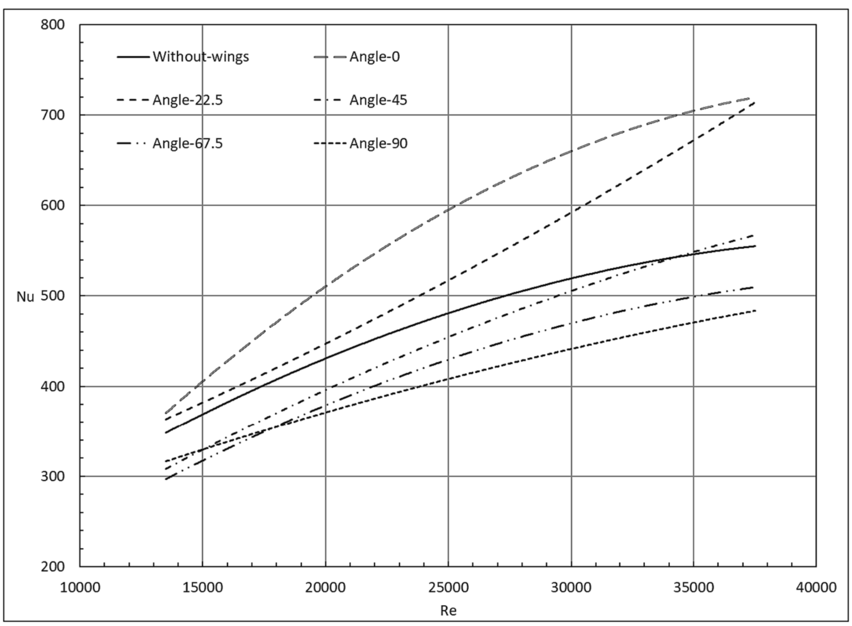

Fig. 5. Nusselt number for **inline arrangement** at different angles of wings.

4. Results and discussion

4.1. Validation of the model

The validation of the model has been carried out through comparing the present work results of Nusselt number and friction factor with the experimental work of Sahin and Demir [17]. The comparison is represented for pin fin heat sink without wings as shown in Fig. 4. The figure shows the same behavior of the Nusselt number and friction factor for experimental and numerical results. Good agreement between experimental and numerical results has been achieved with maximum discrepancy of about 2.16 % in Nusselt number. While the maximum discrepancy in the friction factor is about 12.5 % at the lowest Reynolds number. The thermal losses and measurement errors are assumed reasons for the difference between numerical and experimental results [5].

4.2. Nusselt number and friction factor

Nusselt number is used to present the thermal performance for the studied cases. Fig. 5 represents Nusselt number for inline arrangement at different angles of wings. The maximum Nusselt number has been achieved with angle-0° all over the studied range of Reynolds number. Angles 0 and 22.5 represent enhancement in heat transfer as compared with pin fin heat sink without wings. While angles 45, 67.5, and 90 show lower Nusselt number as compared with case without wings. For staggered arrangement, the maximum Nusselt number is obtained with angle 22.5 as shown in Fig. 6. All studied angles of wings show higher Nusselt number as compared to without wings case. The maximum enhancement achieved in case of inline arrangement is about 31.12 % represented by angle-0 at Re = 37500. While 103.19 % is the maximum enhancement in case of staggered arrangement with angle-22.5 at Re =

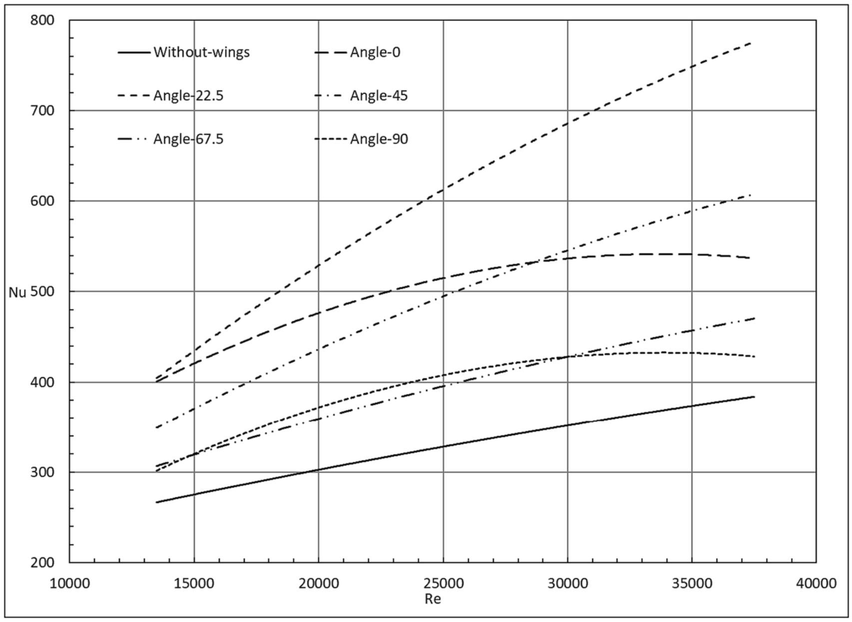

Fig. 6. Nusselt number for **staggered arrangement** at different angles of wings.

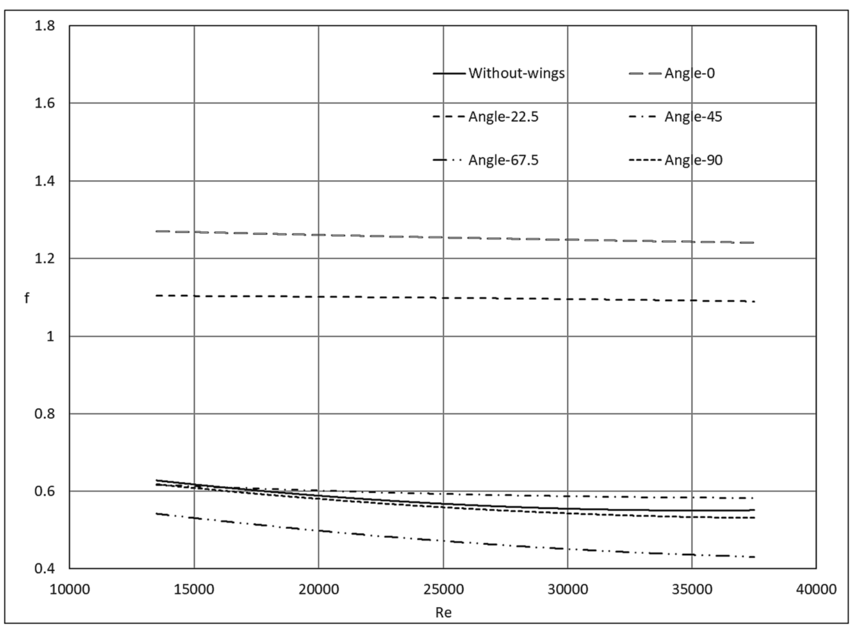

Fig. 7. Friction factor for **inline arrangement** at different angles of wings.

37500. It is noted that the enhancement with staggered arrangement with using wings is higher than that achieved with inline arrangement due to the turbulence occurred by the staggered arrangement. On the other hand, the friction factor is used to represent the pressure drop or the frictional loss through the heat sink. Friction factor for inline arrangement has been represented in Fig. 7. A significant increase in friction factor has been noted for wings with angles 0 and 22.5. This is perhaps due to increase of turbulent intensity. A reduction in friction factor has been obtained with angle 67.5. Fig. 8 also shows a significant increase in friction factor for wings with 0, 22.5, and 45 for staggered arrangement. To understand the behavior of friction factor, Turbulence Kinetic Energy (TKE) has been represented. The turbulence kinetic energy (TKE) is defined as the mean kinetic energy per unit mass. Increasing of turbulence kinetic energy value refers to increase of turbulence level. Presentation of turbulence kinetic energy will explain the increase in Nusselt number and friction factor. Fig. 9 represents the turbulence kinetic energy for the studied cases at Re = 37500. For inline arrangement, the figure shows that the highest TKE is obtained with angle 0°. Wings with angles 67.5° and 90°, is working as a streamed shape for the flow which reduces the TKE in the area between pins. That explains why angles 67.5° and 90° represent lower Nusselt number and friction factor than case without wings. Scattered arrangement by itself increases the turbulence as compared with inline arrangement. Wings with angles 0°, 22.5°, and 45° show higher turbulence specially behind the first row of pin fins. Angle 0° wings push the flow to move densely beside walls, while angle 22.5° increases turbulence of the flow among the second and third rows.

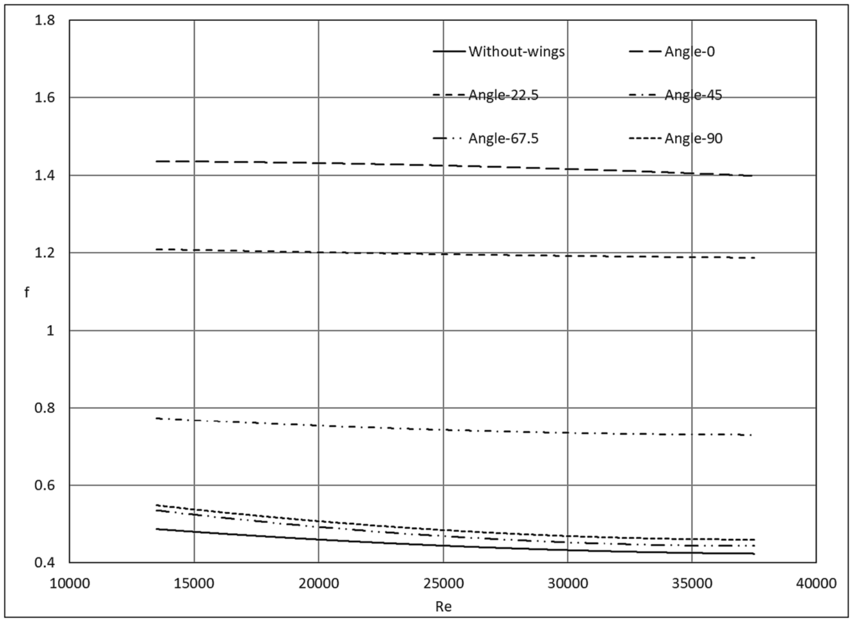

Fig. 8. Friction factor for **staggered arrangement** at different angles of wings.

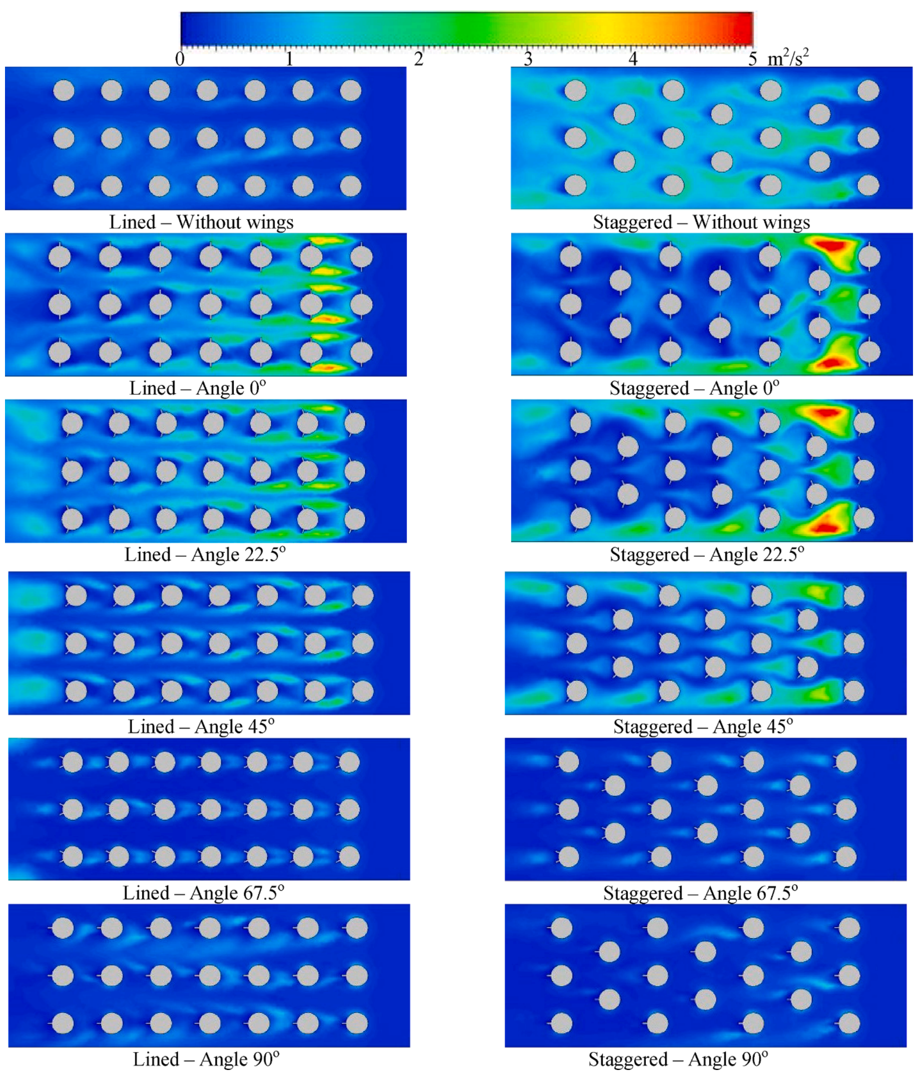

Fig. 9. Turbulence kinetic energy for lined and staggered arrangement at Re = 37500.

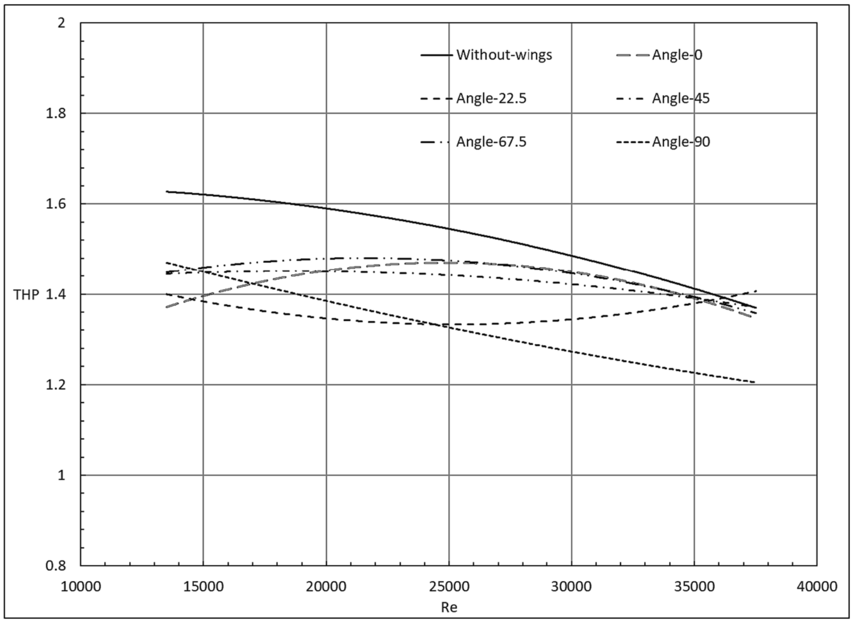

Fig. 10. Thermohydraulic performance for **inline arrangement** at different angles of wings.

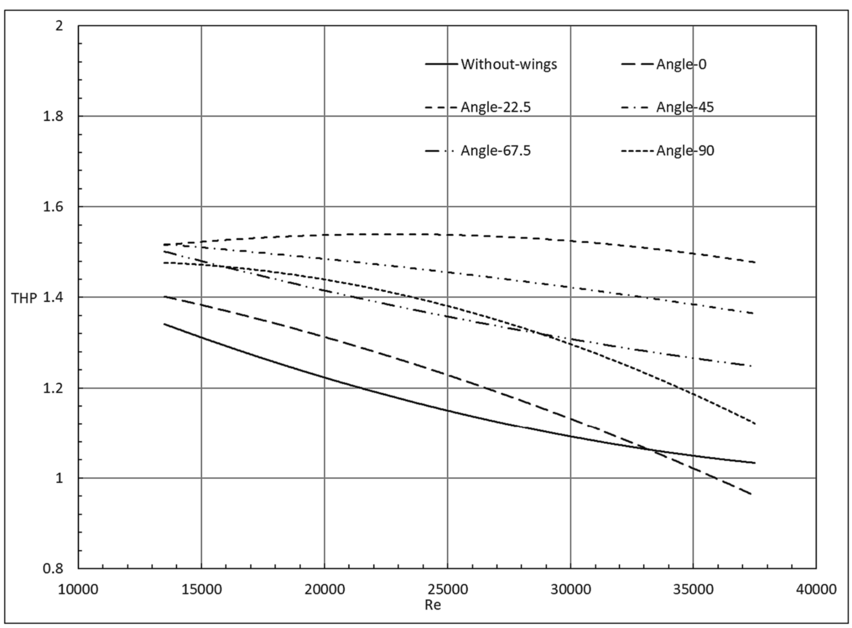

Fig. 11. Thermohydraulic performance for **staggered arrangement** at different angles of wings.

4.3. Thermohydraulic performance (THP)

The main objective of using wings is to increase the heat transfer but on the other hand there will be an increase in pumping power due to increase of friction loss. To obtain the optimum angle of wings, Thermohydraulic performance parameter is used to evaluate the net enhancement in the heat transfer for unit pumping power consumption. Eq. (9) is used to calculate THP [23].

$$THP = \frac{Nu/Nu_s}{(f/f_s)^{1/3}} \tag{9}$$

Where Nu_s and f_s are Nusselt number and friction factor for smooth plate. Eq. (10) is used to calculate Nusselt number for smooth plate [17,23] and Blasius equation is used to calculate the friction factor for smooth plate [23]

$$Nu_s = 0.077Re^{0.716}Pr^{1/3} \tag{10}$$

$$f_s = 0.316Re^{-0.25} \tag{11}$$

Fig. 10 represents the THP for inline arrangement at different angles of wings. The highest value of THP is given by pin fins without wings. While the lowest value is given by angle-90° for high Reynolds number. The Thermohydraulic performance value for other studied angles is around 1.4 for the studied range of Reynolds number. For staggered arrangement, Fig. 11 shows a significant effect of changing the wings angles. Using wings with any angle in staggered arrangement represents improvement in THP except for Re equals 33,000 and 37,000 with 0o angle. The THP without wings at Re = 33000 and 37,500 is higher than THP with wings at 0° as shown in Fig. 11. The highest performance is shown by angle-22.5 while the lowest one is shown by pins without wings. Angle-22.5 shows increasing in THP by about 14.6 % at Re = 13500 and 44 % at Re = 37500 as compared with pin fins without wings. Angle-45 also shows higher THP. It gives the same performance as angle 22.5 at low Reynolds number. But it becomes lower as Reynolds number increases. It can be observed that the optimum angle of the attached wings to the pin fin heat sinks is 22.5° with staggered arrangement. While using pin fins without wings will be the best choice if they arranged inline for the studied range of Re.

5. Conclusion

A numerical study has been carried out to investigate the effect of attaching wings to pin fins heat sinks. Five different angles have been studied and compared with pin fins without wings. Inline and staggered arrangements have been presented for Reynolds numbers ranging from 13,500 to 37500. Nusselt number and friction factor have been used to represent the heat transfer performance and friction loss respectively. For studied range of Reynolds number, The highest Nusselt number has been achieved by angle-0° with inline arrangement while it has been achieved by angle-22.5° with staggered arrangement. On the other hand, the maximum friction factor with both inline and staggered arrangements is represented by angle-0°. To obtain the optimum case at which high heat transfer rate is achieved with low pumping power consumption, Thermohydraulic performance (THP) has been calculated. The results show that the highest thermohydraulic performance has been achieved by angle-22.5° for staggered arrangement while case without wings gives the highest performance for inline arrangement. Using wings in staggered arrangement shows significant effect on heat transfer performance. While it is not recommended to use wings in case of inline arrangement.

Declaration of Competing Interest

The authors declare that they have no known competing financial interests or personal relationships that could have appeared to influence the work reported in this paper.

Acknowledgments

The authors extend their appreciation to the Deanship of Scientific Research at King Khalid University for funding this work through large group Research Project under grant number (RGP2/89/44)

References

[1] Wong KC, Indran S. Impingement heat transfer of a plate fin heat sink with fillet profile. Int J Heat Mass Transf 2013;65: pp. 1-9.
[2] Jeon D, Byon C. Thermal performance of plate fin heat sinks with dual-height fins subject to natural-convection. Int J Heat Mass Transf 2017;113: Oct., p. 1086–92.
[3] Hussain AA, Freegah B, Khalaf BS, Towsyfyan H. Numerical investigation of heat transfer enhancement in plate-fin heat sinks: effect of flow direction and fillet profile. Case Stud Therm Eng 13 2019 Mar; 100388.
[4] Saravanakumara T, Kumar DS. Performance analysis on heat transfer characteristics of Heat SINK with baffles attachment. Int J Therm Sci 2019;142: Aug., p. 14–9.
[5] Abdelmohimen MA, Algarni S, Almutairi K, Ahmed GMS, Irshad K, Irfan SA. Improving heat transfer of plate-fin heat sinks using through rod configurations. ASME J Therm Sci Eng Appl 2021;13: 1, 011003.
[6] Abdelmohimen MAH, Almutairi K, Elkotb MA, Abdelrahman HE, Algarni S. Numerical investigation of using different arrangement of fin slides on the plate-fin heat sink performance. Thermal Science: Year 2021;25(6b):4683–93.
[7] Sparrow EM, Ramsey JW, Altemani CAC. Experiments on in-line pin fin arrays and performance comparison with staggered arrays. ASME J Heat Transfer 1980;102: 44–50.
[8] Tahat M, Kodah ZH, Jarrah BA, Probert SD. Heat transfers from pin-fin arrays experiencing forced convection. Appl Energ 2000;67(4):419–42.
[9] Bilen K, Akyol U, Yapici S. Heat transfer and friction correlations and thermal performance analysis for a finned surface. Energ Convers Manage 2001;42: 1071–83.
[10] Chyu MK. Heat transfer and pressure drop for short pin-fin arrays with pin-endwall fillet. ASME J Heat Transfer 1990;112(9):26–32.
[11] Babus'Haq RF, Akintunde K, Probert SD. Thermal performance of a pin-fin assembly. Int J Heat Fluid Fl 1995;16(1):50–5.
[12] Lau SC, Han JC, Kim YS. Turbulent heat transfer and friction in pin fin channels with lateral flow ejection. ASME J Heat Transfer 1998;111:51–8.
[13] Razelos P, Imre K. The optimal dimensions of circular fins. Trans ASME J Heat Transfer 1980;102:420–6.
[14] Khorunzhii I, Gabor H, Job R, Fahrner WR, Baumann H. Modeling of a pin-fin heat converter with fluid cooling for power semiconductor modules. Int J Energy Res 2003;27:1015–26.
[15] Sahitia N, Lemoueddab A, Stojkovica D, Dursta F, Franzb E. Performance comparison of pin fin in-duct flow arrays with various pin cross-sections. Appl Therm Eng 2006;26:1176–92.
[16] Sara ON. Performance analysis of rectangular ducts with staggered square pin fins. Energ Convers Manage 2003;44(11):1787–803.
[17] Sahin B, Demir A. Thermal performance analysis and optimum design parameters of heat exchanger having perforated pin fins. Energ Conver Manage 2008;49: 1684–95.
[18] Al-Damook A, Kapur N, Summers JL, Thompson HM. An experimental and computational investigation of thermal air flows through perforated pin heat sinks. Appl Therm Eng 2015;89:365–76.
[19] Tijani Alhassan Salami, Binti Jaffri Nursyameera. Thermal analysis of perforated pin-fins heat sink under forced convection condition. Procedia Manuf 2018;24: 290–8.
[20] Naphon P, Sookkasem A. Investigation on heat transfer characteristics of tapered cylinder pin fin heat sinks. Energy Convers Manage 2007;48:2671–9.
[21] Yuan W, Zhao J, Tso CP, Wu T, Liu W, Ming T. Numerical simulation of the thermal hydraulic performance of a plate pin fin heat Sink. Appl Therm Eng 2012;48:81–8.
[22] Sahiti N, Lemouedda A, Stojkovic D, Durst F, Franz E. Performance comparison of pin fin in-duct flow arrays with various pin cross-sections. Appl Therm Eng 2006; 26:1176–92.
[23] Choudhary V, Kumar M, Patil Anil Kumar. Experimental investigation of enhanced performance of pin fin heat sink with wings. Appl Therm Eng 2019;155:546–62.
[24] Souida S, Sahel D, Ameur H, Yousfi A. Numerical simulation of heat transfer behaviors in conical pin fins heat sinks. Acta Mechanica Slovaca 2022;26(3): 32–41.
[25] Bencherif B, Sahel D, Benzeguir R, Ameur H. Performance analysis of central processing unit heat sinks fitted with perforation technique and splitter inserts. J Heat Mass Transfer 2023;145(1):014501.
[26] Bencherif B, Sahel D, Ameur H, Benzeguir R. Investigation of the hydrothermal enhancement of grooved pin fins heat sinks. Int J Ambient Energy 2022;43:1.
[27] Sahel D, Bellahcene L, Yousfi A, Subasi A. Numerical investigation and optimization of a heat sink having hemispherical pin fins. Int Commun Heat Mass Transfer 2021;122:105133.